J Clin Monit Comput (2016) 30:285–294
DOI 10.1007/s10877-015-9716-5

ORIGINAL RESEARCH

Real time noninvasive estimation of work of breathing using facemask leak-corrected tidal volume during noninvasive pressure support: validation study

Michael J. Banner[1] · Carl G. Tams[4] · Neil R. Euliano[4] · Paul J. Stephan[3] · Trevor J. Leavitt[4] · A. Daniel Martin[1,2] · Nawar Al-Rawas[1] · Andrea Gabrielli[1]

Received: 19 November 2014 / Accepted: 5 June 2015 / Published online: 13 June 2015

Abstract We describe a real time, noninvasive method of estimating work of breathing (esophageal balloon not required) during noninvasive pressure support (PS) that uses an artificial neural network (ANN) combined with a leak correction (LC) algorithm, programmed to ignore asynchronous breaths, that corrects for differences in inhaled and exhaled tidal volume (V_T) from facemask leaks ($WOB_{ANN,LC}$/min). Validation studies of $WOB_{ANN,LC}$/min were performed. Using a dedicated and popular noninvasive ventilation ventilator (V60, Philips), in vitro studies using PS (5 and 10 cm H_2O) at various inspiratory flow rate demands were simulated with a lung model. $WOB_{ANN,LC}$/min was compared with the actual work of breathing, determined under conditions of no facemask leaks and estimated using an ANN (WOB_{ANN}/min). Using the same ventilator, an in vivo study of healthy adults (n = 8) receiving combinations of PS (3–10 cm H_2O) and expiratory positive airway pressure was done. $WOB_{ANN,LC}$/min was compared with physiologic work of breathing/min (WOB_{PHYS}/min), determined from changes in esophageal pressure and V_T applied to a Campbell diagram. For the in vitro studies, $WOB_{ANN,LC}$/min and WOB_{ANN}/min ranged from 2.4 to 11.9 J/min and there was an excellent relationship between $WOB_{ANN,LC}$/breath and WOB_{ANN}/breath, $r = 0.99$, $r^2 = 0.98$ ($p < 0.01$). There were essentially no differences between $WOB_{ANN,LC}$/min and WOB_{ANN}/min. For the in vivo study, $WOB_{ANN,LC}$/min and WOB_{PHYS}/min ranged from 3 to 12 J/min and there was an excellent relationship between $WOB_{ANN,LC}$/breath and WOB_{PHYS}/breath, $r = 0.93$, $r^2 = 0.86$ ($p < 0.01$). An ANN combined with a facemask LC algorithm provides noninvasive and valid estimates of work of breathing during noninvasive PS. $WOB_{ANN,LC}$/min, automatically and continuously estimated, may be useful for assessing inspiratory muscle loads and guiding noninvasive PS settings as in a decision support system to appropriately unload inspiratory muscles.

Keywords Work of breathing · Noninvasive · Facemask · Real-time corrections · Tidal volume

1 Introduction

Noninvasive ventilation has been shown to be beneficial in select patients with acute lung injury by improving arterial oxygenation, reducing the need for endotracheal intubation, as well as complications related to intubation, especially ventilator-associated pneumonia, preserving a patient's ability to cough, and improving survival [1, 2]. Goals of noninvasive ventilation include appropriate alveolar ventilation, pulmonary gas exchange, and work of breathing (WOB; the load on inspiratory muscles to spontaneously inhale) [3, 4].

Increased WOB caused by increased elastic loads (lung and chest wall compliance) and/or resistive loads

✉ Michael J. Banner
MBanner@anest.ufl.edu

[1] Department of Anesthesiology, University of Florida College of Medicine, 1600 SW Archer Road, PO Box 100254, Gainesville, FL 32610, USA

[2] Department of Physical Therapy, College of Public Health and Health Professions, University of Florida, Gainesville, FL 32610, USA

[3] Santa Fe College, Gainesville, FL, USA

[4] Convergent Engineering, 107 SW 140th Terrace, #1, Newberry, FL 32669, USA

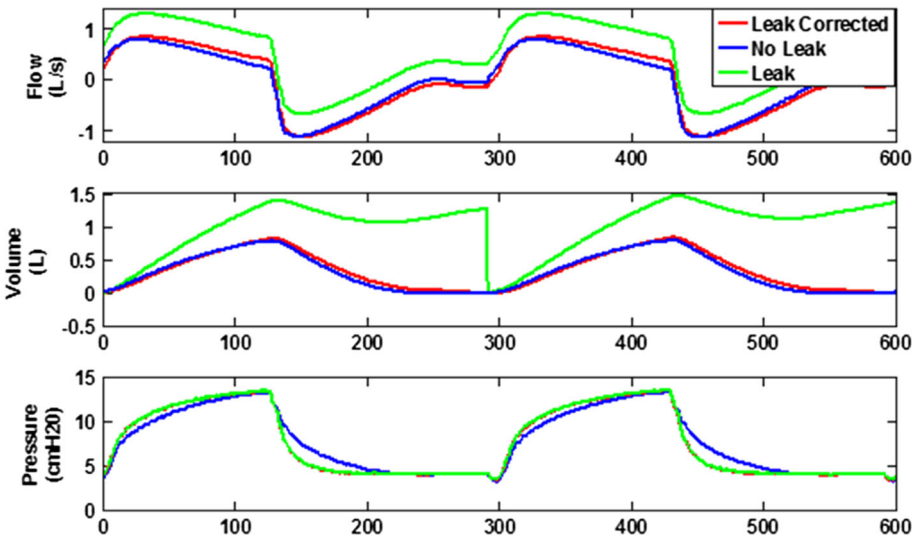

Fig. 1 Facemask leak correction algorithm is shown in operation on facemask flow, tidal volume (V_T), and pressure waveforms during *noninvasive pressure support*, for example 10 cm H_2O with expiratory positive airway pressure at 4 cm H_2O and peak facemask pressure is 14 cm H_2O. Three runs, superimposed on one figure, are shown. First, the control run with no facemask leak is shown (*blue waveforms*). Next, a facemask leak was simulated with no flow correction (*green waveforms*); inspiratory flow rate and V_T are spuriously high. Simultaneously, the facemask leak correction algorithm is shown (*red waveforms*), providing leak corrections of flow, V_T, and pressure. Note that the "No Leak" and "Leak Corrected" waveforms are nearly identical

(physiologic airways resistance) [5] may be assessed by evaluating the breathing pattern; for example, a rapid shallow breathing pattern, dyspnea, and excessive sternocleidomastoid accessory inspiratory muscle contraction. A shortcoming of using the above assessments to infer WOB is that they are qualitative, not quantitative, determinations of inspiratory muscle loads. Qualitative bedside assessments may be somewhat clinician dependent, predisposing to errors in inferring inspiratory muscle loads [6].

Recent advances in the application of artificial neural network (ANN) technology to critical care medicine [7–9] allow WOB per minute to be accurately estimated noninvasively and in real time for intubated patients receiving pressure supported (PS) breaths, obviating an esophageal balloon catheter for determination of esophageal pressure [10]. This approach simplifies assessments of inspiratory muscle loads, allowing practical, clinical use of WOB data at the bedside.

Estimating WOB is predicated on accurate measurement tidal volume (V_T) and being the same during inhalation and exhalation [5, 10]. With facemask leaks [11, 12], and depending on the magnitude of the leak, inhaled V_T may be substantially larger than exhaled V_T, precluding the estimation of WOB. Correcting for facemasks leaks, i.e., exhaled V_T equivalent to inhaled V_T, is needed to estimate WOB. We describe a real time, noninvasive method of estimating work of breathing during noninvasive PS that uses an ANN combined with a leak correction (LC) algorithm that corrects for differences in inhaled and exhaled V_T from facemask leaks ($WOB_{ANN,LC}$/min). We hypothesized that $WOB_{ANN,LC}$/min is a valid estimation of inspiratory muscle loads.

2 Methods

2.1 Leak correction algorithm

Facemask leaks cause a bias flow out of the facemask to the atmosphere, resulting in an upward shift of the flow and volume waveforms during noninvasive PS (Fig. 1). The increased flow causes exhaled V_T to be smaller than it should be, inhaled V_T that is larger than it should be, and a volume curve that "resets" itself after every breath because it does not return to zero (Fig. 1). A leak correction (LC) algorithm that corrects for the facemask leak, as well as flow and V_T waveforms was developed (Convergent Engineering, Gainesville, FL, USA). The LC algorithm applies a two-step process in real time to correct the V_T offset per breath:

Step 1 Flow Conductance through the facemask leak is determined using the following equation:

$$\text{Flow Conductance} = \frac{\sum_{\text{breaths}} \text{flow} * \text{dt}}{\sum_{\text{breaths}} \sqrt{\text{Facemask pressure}}}$$

Step 2 After Flow Conductance is determined, the measured flow waveform is corrected in real time using

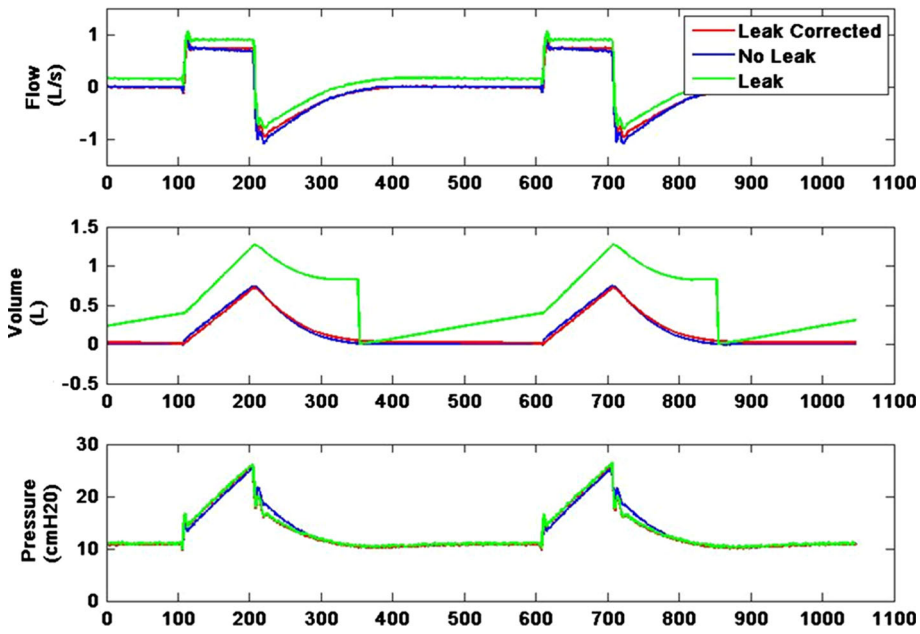

Fig. 2 Facemask leak correction algorithm is shown in operation on facemask flow, tidal volume (V_T), and pressure waveforms for *noninvasive mandatory breaths*. Three runs, superimposed on one figure, are shown. First, the control run with no facemask leak is shown (*blue waveforms*). Next, a facemask leak was simulated with no flow correction (*green waveforms*); inspiratory flow rate and V_T are spuriously high. Simultaneously, the facemask leak correction algorithm is shown (*red waveforms*), providing leak corrections of flow, V_T, and pressure. Note that the "No Leak" and "Leak Corrected" waveforms are nearly identical

the following equation so that the leak corrected V_T may be determined (Figs. 1, 2):

$$\text{Flow}_{\text{Corrected}} = \text{Flow}_{\text{Measured}} - \text{Flow Conductance} \times \sqrt{\text{Facemask pressure}}.$$

While developing the LC algorithm that is combined with the ANN, it was realized breathing asynchrony confounded estimated work of breathing values. Accordingly, by using pressure and flow waveform tracings, software was written to identify different types of breathing asynchrony as described by Vignaux et al. [13], i.e., ineffective breaths, double triggering, auto-triggering, premature cycling, and late cycling and ignore these breaths. The key point is the ANN estimates work of breathing using only breaths that are in *synchrony* with the ventilator. Thus, the aforementioned forms of breathing asynchrony do not affect the estimated values for work of breathing.

Two in vitro studies were done using a two-lung compartment model (TTL, Michigan Instruments, Grand Rapids, MI, USA) composed of a driving lung inflated by a ventilator (Puritan-Bennett 7200, Covidien, Dublin, Ireland) that simulated inspiratory muscles, which caused a second lung that simulated a patient lung, to inhale (Fig. 3). Compliance was decreased from the normal adult value of 0.1 L/cm H_2O to 0.05 L/cm H_2O (50 % decrease) and resistance was increased from the normal value of 2 cm H_2O/L/s to 5 cm H_2O/L/s (150 % increase). This was done to simulate a patient with a degree of compromised pulmonary mechanics associated with increased elastic and resistive work of breathing. Spontaneous V_T of 0.4 L, breathing frequency of 20/min, and sinusoidal peak inspiratory flow rate (PFR) demands of 30 and 60 L/min were set by adjusting the ventilator of the driving lung (Fig. 3). These parameters were chosen because they are similar to those used for evaluative research [4, 12]. Via a facemask (Performax mask, Philips, Murrysville, PA, USA) attached to a model of a face and head, a noninvasive ventilation ventilator (V60, Philips) was connected to the patient lung. A calibrated and fairly stable leak flow rate of approximately 20 L/min at driving pressures of 10–15 cm H_2O (akin to facemask pressures used in the study) was created by drilling an appropriately sized hole in an adapter placed between the facemask and end of the ventilator breathing circuit tubing. This leak flow rate is in accordance with reported ranges of facemask leak flow rates that have been evaluated for use with noninvasive ventilation [11, 12]. The facemask leak flow rate was recorded from the value displayed on the ventilator (displayed as "Patient Leak"); this is the same procedure that is done clinically. As described in the ventilator's operating manual, this value is estimated after entering a calibration factor into the ventilator on start-up which allows the ventilator to estimate the intentional leak flow rate through the exhalation port and ports on the facemask. From an algorithm, it estimates the total leak flow rate, the sum of intentional leak flow rate and facemask or unintentional leak flow rate. Facemask leak flow rate is then estimated as the difference in total leak flow rate and intentional leak flow rate.

Noninvasive PS at 5 and 10 cm H_2O with expiratory positive airway pressure (EPAP) at 5 cm H_2O were applied, similar to settings previously used [4, 12]. A pressure/flow sensor, connected to the facemask at the end

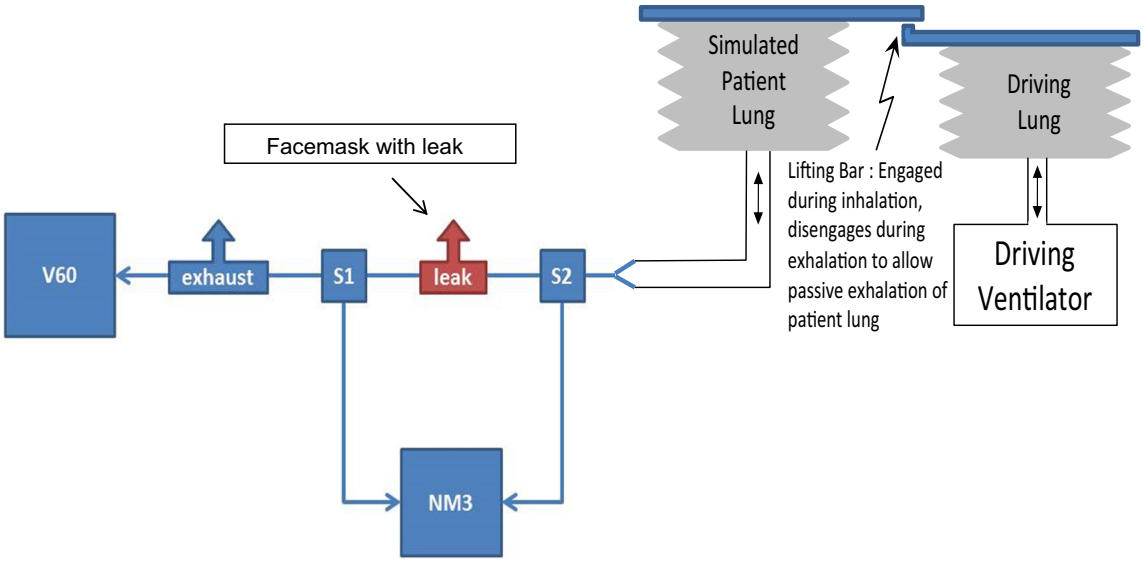

Fig. 3 In vitro model used to simulate spontaneous breathing is shown. The driving lung on the right simulates a patient's inspiratory muscles by driving/lifting a patient lung on left. A noninvasive ventilator (V60, Philips) was set to provide various levels of noninvasive pressure support and expiratory positive airway pressure (see Sect. 2). A facemask with a leak was positioned between pressure and flow sensors at Site 1 (S1) and Site 2 (S2). Data from the sensors were directed to a respiratory monitor (NM3, Philips). Tidal volume at S1, proximal to the facemask leak, was determined using leak-correction algorithm software in a laptop computer connected to the monitor (not shown), which in turn, was used to determine noninvasive, leak-corrected work of breathing/min using artificial neural network software. The actual work of breathing per minute was also determined using artificial neural network software at S2, distal to the leak; at this site inhaled and exhaled tidal volume were essentially the same and were unaffected by the leak

of the ventilator breathing tubing at Site 1, and another pressure/flow sensor, positioned after the facemask and before the patient lung at Site 2 (Fig. 3), directed data to a respiratory monitor (NM3, Philips) and laptop computer containing ANN WOB software [10] (see "Appendix") and the aforementioned LC algorithm software. At Site 1, the algorithm measures the differences in inhaled and exhaled V_T (facemask leak) and applies the LC software to determine the corrected V_T allowing $WOB_{ANN,LC}$/min to be estimated. At Site 2, inhaled and exhaled V_T were equivalent because at this site, there was is no flow leakage to adversely affect the pressure, flow, and volume waveforms. WOB at this site, also estimated using the ANN software [10], was the actual work of breathing per minute (WOB_{ANN}/min). $WOB_{ANN,LC}$/min data were compared to WOB_{ANN}/min data to validate estimations of $WOB_{ANN,LC}$/min.

The second in vitro study was performed at PS 10 cm H_2O and EPAP 5 cm H_2O, common settings that have been reported [4, 12]. Employing the same model as above, PFR demands of 30, 50, 65, and 75 L/min were simulated. The same monitoring and methods of determining the leak-corrected V_T, $WOB_{ANN,LC}$/min, and WOB_{ANN}/min as previously described were used for this study. $WOB_{ANN,LC}$/min and per breath data were compared to WOB_{ANN}/min and per breath data.

An in vivo study was performed with IRB approval, and after obtaining informed consent from healthy adults ($n = 8$, 8 males, weight 187 ± 23 lbs, age 38 ± 8 years). PS ranging from 3 to 10 cm H_2O with EPAP from 4 to 5 cm H_2O was applied with a noninvasive ventilator (V60, Philips). Subjects were coached to breathe at two frequencies, at approximately 10 breaths/min and then at approximately 20 breaths/min. Breathing at different frequencies is associated with different peak flowrate demands and values for work of breathing. This was purposely done to vary facemask leak flowrates and PFR demands which were needed to assess estimates of $WOB_{ANN,LC}$/min. A combined pressure/flow sensor, positioned between the facemask (Performax mask, Philips) and the end of the ventilator breathing tubing, directed data to respiratory monitor (NM3, Philips) and laptop computer containing the ANN WOB software [10] and LC algorithm software (Convergent Engineering, Gainesville, FL, USA). An esophageal balloon catheter was orally inserted into the esophagus and appropriately positioned using the occlusion test [14]. Changes in Pes were integrated with changes in V_T, obtained from the V_T LC algorithm, to form a Pes V_T loop that, in turn, was applied to a Campbell diagram for determination WOB per breath. These data were averaged over 1 min for determination of physiologic work of breathing per minute (WOB_{PHYS}/min), i.e., the reference WOB

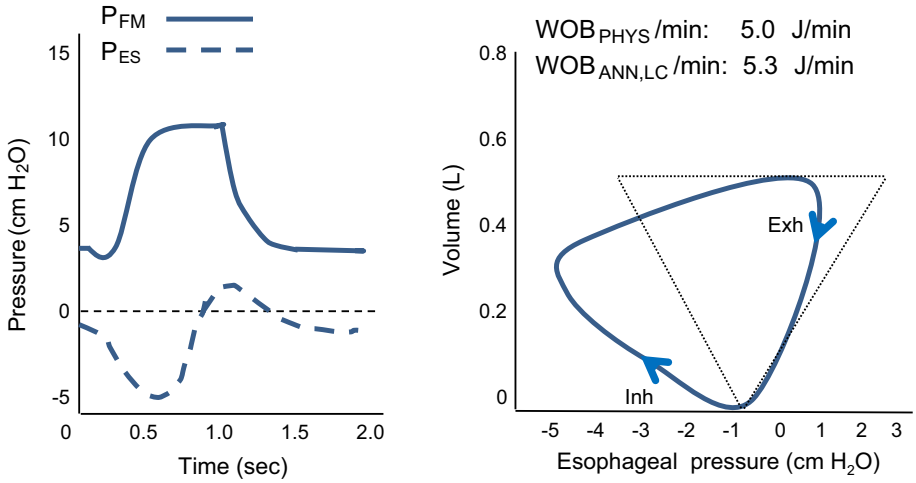

Fig. 4 Changes in facemask (P_{FM}) and esophageal pressures (P_{ES}) are shown (*left*) with the associated Campbell diagram, which was used to determine physiologic work of breathing (WOB_{PHYS}/min) (*right*) for a subject receiving noninvasive pressure support 6 cm H_2O with expiratory positive airway pressure at 4 cm H_2O (*Inh* inhalation, *Exh* exhalation). For this condition, work of breathing estimated noninvasively using an artificial neural network (ANN) combined with a facemask leak correction (LC) algorithm ($WOB_{ANN,LC}$/min) was comparable to WOB_{PHYS}/min

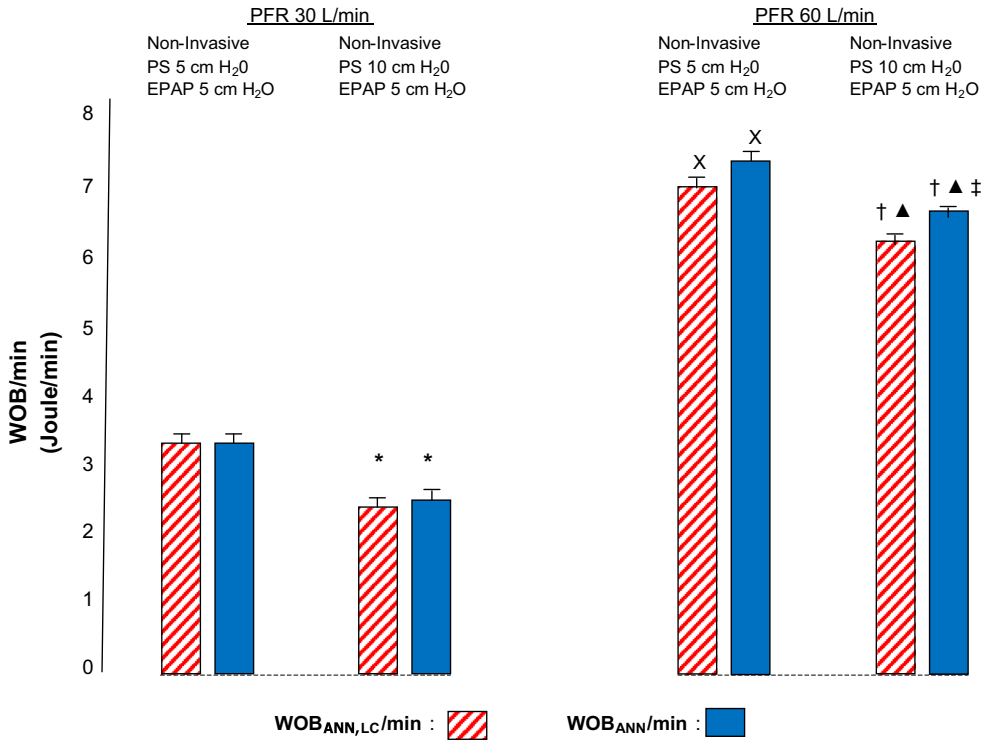

Fig. 5 Where $WOB_{ANN,LC}$/min work of breathing estimated noninvasively using an artificial neural network (ANN) combined with a facemask leak correction (LC) algorithm and WOB_{ANN}/min is the actual work of breathing per minute estimated from the ANN and not affected by facemask leaks. $p < 0.05$ compared to noninvasive pressure support (PS) 5 cm H_2O at a peak flow rate (PFR) demand of 30 L/min (*asterisk symbols*); compared to noninvasive PS 5 cm H_2O at PFR 60 L/min (*dagger symbols*); compared to noninvasive PS 5 cm H_2O at PFR demand 30 L/min (X); compared to noninvasive PS 10 cm H_2O at PFR demand of 30 L/min (*triangle symbols*); compared to $WOB_{ANN,LC}$/min at PFR demand of 60 L/min during noninvasive PS 10 cm H_2O (*double dagger symbols*). Data are mean ± SD

(Fig. 4). Chest wall compliance for the Campbell diagram was set at a normal value of 0.2 L/cm H_2O [5]. Simultaneously, the same V_T as obtained from the LC algorithm used for determining WOB_{PHYS}/min was also used for estimating $WOB_{ANN,LC}$/min with the ANN WOB software [10]. WOB_{PHYS}/min and per breath data were compared

with $WOB_{ANN,LC}$/min and per breath. All data were analyzed with ANOVA, regression, and Bland–Altman analyses; alpha was set a 0.05 for statistical significance.

3 Results

For the first in vitro study, WOB values ranged from 2.4 to 7.6 J/min. At a PFR demand of 30 L/min during noninvasive PS 5 and 10 cm H_2O, there were no differences between $WOB_{ANN,LC}$/min and WOB_{ANN}/min (Fig. 5). At a PFR demand of 60 L/min during noninvasive PS 5, there were no differences between $WOB_{ANN,LC}$/min and WOB_{ANN}/min (Fig. 5); during noninvasive PS 10 cm H_2O, $WOB_{ANN,LC}$/min was 6.2 ± 0.09 J/min and WOB_{ANN}/min was 6.7 ± 0.05 J/min ($p < 0.05$). At a PFR demand of 30 L/min during noninvasive PS 5 cm H_2O compared to noninvasive PS 10 cm H_2O, $WOB_{ANN,LC}$/min and WOB_{ANN}/min decreased significantly from an average of 3.3–2.4 J/min ($p < 0.05$), a 27.3 % decrease (Fig. 5). Similarly, At a PFR demand of 60 L/min during noninvasive PS 5 cm H_2O compared to noninvasive PS 10 cm H_2O, $WOB_{ANN,LC}$/min and WOB_{ANN}/min decreased significantly from an average of 7.05–6.45 J/min ($p < 0.05$), an 8.5 % decrease (Fig. 5). At a PFR demand of 60 L/min during noninvasive PS 5 and 10 cm H_2O compared to a PFR demand of 30 L/min during noninvasive PS 5 and 10 cm H_2O, $WOB_{ANN,LC}$/min and WOB_{ANN}/min were significantly higher (Fig. 5).

For the second in vitro study, $WOB_{ANN,LC}$/min and WOB_{ANN}/min values ranged from 2.6 to 11.9 J/min. $WOB_{ANN,LC}$/breath correlated with increases and decreases in WOB_{ANN}/breath at the different PFR demands, i.e., as PFR demands increased, WOB increased and vice versa. The relationship between $WOB_{ANN,LC}$/breath and WOB_{ANN}/breath at all PFR demands was positive and very strong, $r = 0.99$, $r^2 = 0.98$ ($p < 0.01$) (Fig. 6a). Bias was slightly negative and small at −0.15 J/breath, precision was small at ±0.26, and the limits of agreement was ±0.53 (Fig. 6b).

For the in vivo study, V_T ranged from 0.4 to 0.75 L, breathing frequency ranged from 12 to 22 breaths/min, and PFR demands ranged from 20 to 60 L/min. Facemask leak flow rates were 13.5 ± 8.7 L/min; in accordance with reported clinical values (Table 1) [12]. $WOB_{ANN,LC}$/min and WOB_{PHYS}/min values ranged from 3 to 12 J/min. $WOB_{ANN,LC}$/breath correlated with increases and decreases in WOB_{PHYS}/breath at different levels of noninvasive PS. The relationship was positive and strong, $r = 0.93$, $r^2 = 0.86$ ($p < 0.01$) (Fig. 7a). Bias was small at −0.01 J/breath, precision was ±0.07 J/min, and the limits of agreement was ±0.15 (Fig. 7b).

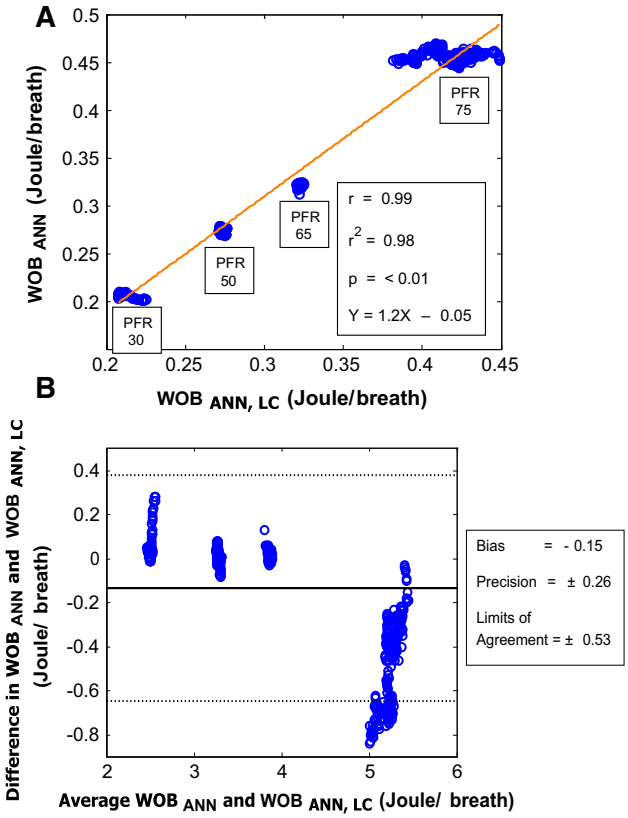

Fig. 6 **a** Relationship of in vitro actual work of breathing per breath estimated from an artificial neural network (ANN) and not affected by facemask leaks (WOB_{ANN}/breath) and work of breathing estimated noninvasively using an artificial neural network (ANN) combined with a facemask leak correction (LC) algorithm ($WOB_{ANN,LC}$/breath) at simulated spontaneous peak inspiratory flow rate (PFR) demands of 30, 50, 65, and 75 L/min during noninvasive pressure support at 10 cm H_2O and expiratory positive airway pressure at 5 cm H_2O; commonly used settings is shown. (Multiple points are clustered at each PFR condition, causing the amorphous-appearing shapes). **b** Corresponding Bland–Altman plot for (**a**) is shown, note bias and precision values

4 Discussion

The primary finding of this research is that WOB estimated using an ANN combined with a LC algorithm provided valid estimations of WOB during noninvasive PS. The findings appear to be clinically relevant because WOB values in this study ranged from approximately 2–12 J/min—typical of values we have observed while treating adults with respiratory failure for 20 years. For the in vitro studies, essentially no differences were found comparing $WOB_{ANN,LC}$/min to WOB_{ANN}/min at different levels of noninvasive PS or at higher and lower PFR demands. Although small statistical differences between $WOB_{ANN,LC}$/min and WOB_{ANN}/min were found

Table 1 Facemask leak flow rates during noninvasive pressure support (adult subjects)

Subject	Leak flow rate (L/min)
1	9
2	8
3	10
4	16
5	34
6	12
7	8
8	11
	13.5 ± 8.7

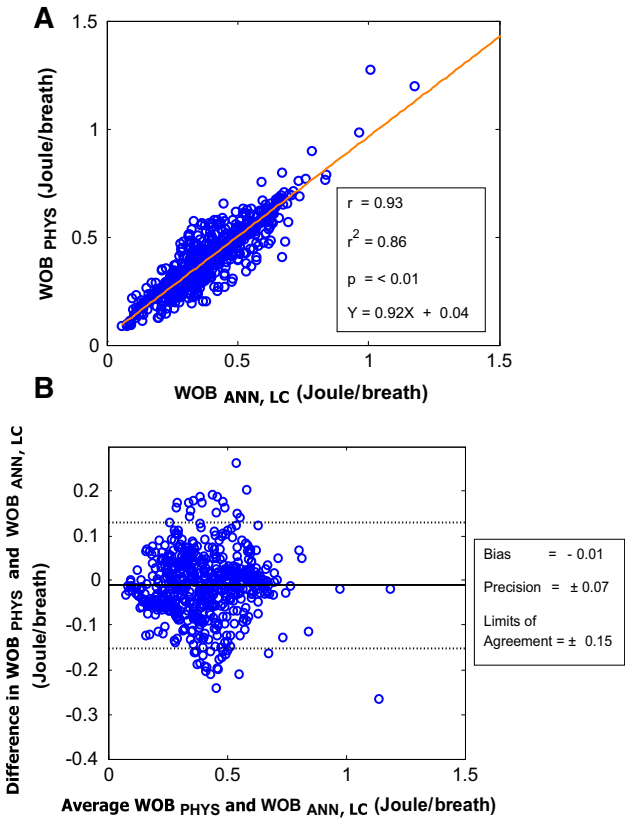

Fig. 7 **a** Relationship of in vivo physiologic work of breathing per breath (WOB_{PHYS}/breath) and work of breathing estimated noninvasively using an artificial neural network (ANN) combined with a facemask leak correction (LC) algorithm ($WOB_{ANN,LC}$/breath) at various combinations of noninvasive pressure support and expiratory positive airway pressure in adults is shown. **b** Corresponding Bland–Altman plot for (**a**) is shown, note bias and precision values

during one test condition, a 0.5 J/min difference, this was not considered to be clinically significant. As noninvasive PS was increased, $WOB_{ANN,LC}$/min and WOB_{ANN}/min decreased, and vice versa. As PFR demands increased, $WOB_{ANN,LC}$/min and WOB_{ANN}/min increased by similar amounts, most likely due to increases in resistive WOB, not elastic WOB because V_T was essentially unchanged with the mechanical model. A highly significant relationship was found between $WOB_{ANN,LC}$/breath and WOB_{ANN}/breath and $WOB_{ANN,LC}$/breath predicted or explained 98 % of variance in WOB_{ANN}/breath, an excellent predictor of WOB_{ANN}/breath ($p < 0.01$). A slight negative bias of −0.15 J/breath for $WOB_{ANN,LC}$/min was found and considered to be negligible, whereas precision was small at ±0.26 and deemed clinically acceptable. For the in vivo study, $WOB_{ANN,LC}$/breath correlated highly with WOB_{PHYS}/breath at various levels of noninvasive PS. For the range of noninvasive PS used, as WOB_{PHYS}/breath increased and decreased, $WOB_{ANN,LC}$/breath changed in the same manner. A significant relationship was found between $WOB_{ANN,LC}$/breath and WOB_{PHYS}/breath and $WOB_{ANN,LC}$/breath predicted or explained 86 % of variance in WOB_{PHYS}/breath, a very good predictor of WOB_{PHYS}/breath ($p < 0.01$). Regarding the remaining 14 % of the variance, factors explaining this variance are unclear. It may be related to equipment calibrations of the various pieces of equipment used. A small negative bias of −0.01 J/breath for $WOB_{ANN,LC}$/min was negligible, whereas precision was small at ±0.07 and deemed clinically acceptable.

A goal of noninvasive PS for patients with respiratory insufficiency is to unload inspiratory muscles, which allows patients to breathe easier and to help relieve dyspnea. WOB and patient effort decreased on average by 60 % at inspiratory PS settings of approximately 15 cm H_2O and there were near uniform decreases in dyspnea scores [15]. At noninvasive ventilation settings that provided maximum efficacy, WOB was reduced to a range of 5.4–10.2 J/min (essentially the normal adult range) [4, 16–18]. In patients with acute lung injury, noninvasive PS was shown to reduce neuromuscular drive, unload inspiratory muscles, and improve dyspnea [4]. In that study, WOB/min and transdiaphragmatic pressure decreased significantly from 8.7 to 6.5 J/min (25.3 % decrease) and from 10.3 to 5.8 cm H_2O (43.6 % decrease), respectively, as noninvasive PS was increased from continuous positive airway pressure [4]. These findings are in accordance with intubated patients receiving PS [19].

The aforementioned studies provide clues as to how $WOB_{ANN,LC}$/min data may be useful for treating patients receiving noninvasive PS; for example, by assessing inspiratory muscle loads and guiding ventilator settings to appropriately unload inspiratory muscles. Applying insufficient or not enough noninvasive PS predisposes to abnormally increased values of WOB and inspiratory muscle fatigue [19], while applying too high a level of noninvasive PS over a long time is associated with abnormally low values of WOB and may predispose to disuse atrophy [19]. Unloading the inspiratory muscles so that the WOB/min for adults is in a clinically tolerable

adult range of approximately 5–10 J/min [6, 20] may be an appropriate goal for setting noninvasive PS.

Real time monitoring of $WOB_{ANN,LC}$/min may also allow clinicians to determine a proper rate of inspiratory pressure rise setting during noninvasive PS, i.e., while at a specific PS level, set the rate of inspiratory pressure rise to achieve an appropriate $WOB_{ANN,LC}$/min. Many noninvasive ventilators permit a range of inspiratory pressure rise settings. The rate of pressurization to a preselected noninvasive PS level is related to the interaction of the noninvasive ventilator's flow rate output and the patient's inspiratory flow rate demand. When using a slower rate of inspiratory pressure rise setting, the noninvasive ventilator's flow rate output may be substantially less than the patient's inspiratory flow rate demand, resulting in a slow pressure rise time; this is associated with increased WOB and patient discomfort [21]. Conversely, when using a faster rate of inspiratory pressure rise setting, the noninvasive ventilator's flow rate output may better match the patient's inspiratory flow rate demand, resulting in a rapid pressure rise time, associated with lower work of breathing, leading to improved comfort [21].

Our ANN with LC algorithm for estimations of work of breathing was functional for the facemask leak flow range in this study, i.e., up to 34 L/min, which is in excess of reported values in clinical practice using noninvasive PS [12, 13]. It has been reported that facemask leaks >40 L/min are likely to impair the efficiency of ventilators used to provide noninvasive ventilation [22]. Although not evaluated at leak flow rates ≥40 L/min, we speculate that such large facemask leak flow rates may also compromise the functionality of our LC algorithm.

Limitations of the study may be that fairly commonly applied levels of noninvasive PS and EPAP were used. To study all possible combinations of noninvasive PS and EPAP we speculate may have achieved findings comparable to those revealed in this study. A second limitation is that it is unclear if a ventilator other than the dedicated noninvasive ventilation ventilator used in the study affects the findings. Another potential limitation is that part of the study was conducted using a human patient simulation, raising the concern of clinical relevancy. The simulated pulmonary mechanics chosen, as well as the range of WOB values measured were comparable to conditions treating adults with respiratory insufficiency, suggesting that the findings may be relevant for patients receiving noninvasive PS. A clinical study using our method of estimating work of breathing on patients treated with noninvasive PS with respiratory failure, with and without chronic obstructive pulmonary disease, is recommended.

In summary, an LC algorithm, programmed to ignore asynchronous breaths, directs pressure, flow, and tidal volume data to an ANN to provide noninvasive and valid estimates of work of breathing during noninvasive PS. $WOB_{ANN,LC}$/min, estimated automatically and continuously, may be useful in a decision support system for assessing inspiratory muscle loads and guiding noninvasive PS settings to unload inspiratory muscles.

Acknowledgments This work was supported by institutional/departmental funds and by Philips/Respironics, Inc.

Conflict of interest Dr. Banner is a consultant for Convergent Engineering, developer of software used in the study. Dr. Euliano, President of Convergent Engineering, wrote software used in the study.

Appendix: Artificial neural network for estimating noninvasive work of breathing (previously published[10])

Five predictor variables/input elements, used in a multilayer perceptron artificial neural network (ANN) model (figure below), found to be highly correlated with noninvasive work of breathing (WOB) per minute, were chosen because they produced the best (lowest mean squared error) possible predictive value. Incorporating inputs in addition to those five variables did not increase predictive performance, thus this set was considered sufficient for predicting/calculating noninvasive WOB per minute. (1) *Minute ventilation*, the spontaneous minute ventilation (not including mandatory breaths), was found to be closely tied to noninvasive WOB per minute; the larger the minute ventilation, the greater the workload and vice versa. (2) *Intrinsic positive end expiratory pressure (PEEPi)*, is the parameter estimated from the exhalation portion of a flow-volume loop. In patients for whom PEEPi was suspected, we observed that exhaled flow did not reset/return to zero but to some discrete value at end-exhalation on a flow-volume loop. By linearly extrapolating this value to the zero flow axis on the flow-volume loop, an estimate of air trapping or excess volume remaining in the lungs at end-exhalation is made. By knowing this volume and respiratory system compliance, a pressure is calculated (pressure = volume/compliance), a reflection of PEEPi. The larger the estimated PEEPi value, the larger the workload and vice versa. Respiratory system compliance and resistance were estimated in real time using the expiratory time constant method (Al-Rawas et al., Expiratory time constant for determinations of plateau pressure, respiratory system compliance, and total resistance. *Critical Care* 2013; 17: R23). (3) *Airway pressure trigger depth* is a parameter that measured the decrease in pressure below baseline airway pressure (Paw) at the Y-piece of the breathing circuit just before the ventilator triggers "ON." Large inspiratory efforts tend to decrease this pressure more rapidly, causing

a large decrease in pressure or trigger pressure depth. The larger the decreases in trigger pressure depth, the larger the workload and vice versa. (4) *Inspiratory rate of flow rise* is the parameter that assessed how rapidly the inspiratory flow waveform rose during a pressure supported breath. An actively breathing patient with a strong inspiratory effort and demanding a high flow rate from the ventilator tends to display a rounded or sinusoidal-shaped inspiratory flow profile; peak flow occurs during the mid to latter portion of the breath. It takes a longer time for flow to reach maximum during inhalation. In contrast, a patient who inhales passively while receiving a pressure-supported breath typically displays a rapid rise in flow very early in the breath. Flow reaches maximum at nearly the onset of the breath in a very brief time and then decelerates for the remainder of inhalation. A coded value for inspiratory rate of flow rise was devised to range from zero to one. The higher the value, the more rounded or sinusoidal the inspiratory flow profile, and the greater the workload. The lower the value, the more a decelerating inspiratory flow profile, and the lower the workload. (5) *Pmus* is the respiratory muscle pressure; it is the sum of elastic and resistive pressures and was determined using the equation of motion, i.e., Pmus + Paw = (tidal volume/respiratory system compliance) + (respiratory system resistance × inspiratory flow rate). This is a reflection of the pressure generated by the inspiratory muscles during spontaneous inhalation; the larger the value, the larger the estimated effort to inhale and vice versa.

References

1. Brochard L, Mancebo J, Wysocki M, Lofaso F, Conti G, Rauss A, Simonneau G, Benito S, Gasparetto A, Lemaire F, Isabey D, Harf A. Noninvasive ventilation for acute exacerbations of chronic obstructive pulmonary disease. NEJM. 1995;333:817–22.
2. Bernstein AD, Holt AW, Vedig AE, Skowronski GA, Baggoley CJ. Treatment of severe cardiogenic pulmonary edema with continuous positive airway pressure delivered by facemask. NEJM. 1991;325:1825–30.
3. Garpestad E, Brennan J, Hill NS. Noninvasive ventilation for critical care. Chest. 2007;132(2):711–20.
4. L'Her E, Deye N, Lellouche F, Taille S, Demoule A, Fraticelli A, Mancebo J, Brochard L. Physiologic effects of noninvasive ventilation during acute lung injury. Am J Resp Crit Care Med. 2005;172:1112–8.
5. Millic-Emilli J. Work of breathing. In: Crystal RG, West JB, editors. The lung. New York: Raven Press; 1991. p. 1065–75.
6. Kirton OC, DeHaven CB, Hudson-Civetta J, Morgan JP, Windsor J, Civetta JM. Re-engineering ventilator support to decrease days and improve resource utilization. Ann Surg. 1996;224(3):396–404.
7. Baxt WG. Application of artificial neural networks to clinical medicine. Lancet. 1995;346:1135–8.
8. Rodvold DM, McLoad DG, Brandt JM, Snow PB, Murphy GP. Introduction to artificial neural networks for physicians: taking the lid off the blackbox. Prostate. 2001;46:39–44.
9. Leon MA, Lorini FL. Ventilation mode recognition using artificial neural networks. Comp Biomed Res. 1997;30:373–8.
10. Banner MJ, Euliano NR, Brennan V, Peters C, Layon AJ, Gabrielli A. Power of breathing determined noninvasively with use of an artificial neural network in patients with respiratory failure. Crit Care Med. 2006;34:1052–9.
11. Oto J, Chenelle CT, Marchase AD, Kacmarek RM. A comparison of leak compensation in acute care ventilators during non-

Model of Artificial Neural Network (multilayer perceptron) used for estimating noninvasive work of breathing per minute

Five input elements (left side), eight processing elements (center), and one output processing element (right side) are contained within three layers of the model. * Synapses represent trainable weights that contain the "intelligence" of the system.

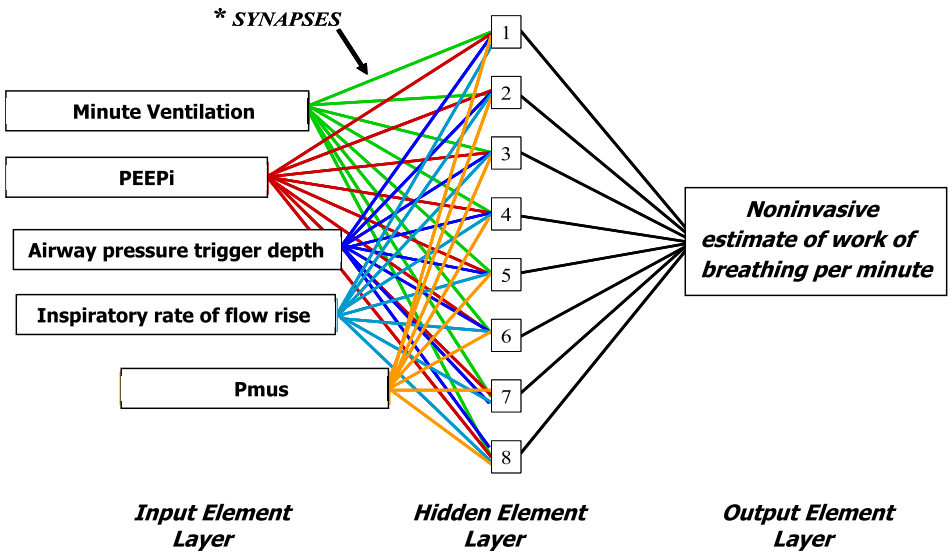

invasive and invasive ventilation: a lung model study. Resp Care. 2013;58(12):2027–37.
12. Carteaux G, Lyazidi A, Cordoba-Izqierdo A, Vagnauz L, Jolliet P, Thille AW, Richard JM, Brochard L. Patient-ventilator asynchrony during noninvasive ventilation. Chest. 2012;142:367–76.
13. Vignaux L, Vargas F, Roeseler J, Tassaux D, Thille AW, Kossowsky MP, Brochard L, Jolliet P. Patient-ventilator asynchrony during non-invasive ventilation for acute respiratory failure: a multicenter study. Intensive Care Med. 2009;35:840–6.
14. Baydur A, Behrakis PK, Zin WA, Jaeger M, Milic-Emili J. A simple method for assessing the validity of the esophageal balloon technique. Am Rev Respir Dis. 1982;126:788–91.
15. Kallet RH, Diaz JV. The physiologic effects of noninvasive ventilation. Resp Care. 2009;54(1):102–14.
16. Girault C, Richard JC, Chevron V, Tamion F, Pasquis P, Leroy J, Bonmarchand G. Comparative physiologic effects of non-invasive assist control and pressure support ventilation in acute hypercapnic respiratory failure. Chest. 1997;111(6):1639–48.
17. Vanpee D, El Kawand C, Rousseau L, Jamart J, Delaunois L. Effects of nasal pressure support on ventilation and inspiratory work in normocapnic and hypercapnic patients with stable COPD. Chest. 2002;122(1):75–83.
18. Lellouche F, L'Her E, Abroug F, Deye N, Rodriguez PO, Rabbat A, Jaber S, Fartoukh M, Conti G, Cracco C, Richard JC, Ricard JD, Mal H, Mentec H, Loisel F, Lacherade JC, Taillé S, Brochard L. Effects of humidification device on the work of breathing during noninvasive ventilation. Intensive Care Med. 2002;28(11):1582–9.
19. Brochard L, Harf A, Lorino H, Lemaire F. Inspiratory pressure support prevents diaphragmatic fatigue during weaning from mechanical ventilation. Am Rev Respir Dis. 1989;139:513–21.
20. Banner MJ, Euliano NR, Martin AD, Al-Rawas N, Layon AJ, Gabrielli A. Noninvasive work of breathing improves prediction of post-extubation outcome. Intensive Care Med. 2012;38(2):248–55.
21. Prinianakis G, Delmastro M, Carlucci A. Effect of varying the pressurization rate during non-invasive pressure support ventilation. Eur Respir J. 2004;23:314–20.
22. Borel JC, Sabil A, Janssens JP, Couteau M, Boulon L, Levy P, Pepin JL. Intentional leaks in industrial masks have a significant impact on the efficacy of bi-level non-invasive ventilation. Chest. 2009;135:669–77.